SAKARYA UNIVERSITY JOURNAL OF COMPUTER AND INFORMATION SCIENCES
http://saucis.sakarya.edu.tr/
e-ISSN: 2636-8129
Publisher: Sakarya University
Vol. 7, No. 3, 2024, 439-448
DOI: 10.35377/saucis...1522290
SAUCIS
SAKARYA UNIVERSITY

RESEARCH ARTICLE

Enhancing Fall Detection Accuracy: The Ground-Face Coordinate System for 3D Accelerometer Data

Abdullah Talha Sözer

Karabuk University, Faculty of Engineering, Electrical and Electronics Engineering Department, Karabuk, Türkiye

Corresponding author:
Abdullah Talha Sözer,
Karabuk University, Faculty of Engineering, Electrical and Electronics Engineering Department, Karabuk, Türkiye
talhasozer@karabuk.edu.tr

Article History:
Received: 25.07.2024
Accepted: 21.10.2024
Published Online: 24.12.2024

ABSTRACT
The global elderly population is on the rise, leading to increased physical, sensory, and cognitive changes that heighten the risk of falls. Consequently, fall detection (FD) has emerged as a significant concern, attracting considerable attention in recent years. Utilizing 3D accelerometer sensors for FD offers advantages such as cost-effectiveness and ease of implementation; however, traditional raw 3D accelerometer signals are inherently dependent on the device's orientation and placement within the device coordinate system. Misalignment between the device's axes and the direction of movement can lead to misinterpretation of acceleration signals, potentially causing misclassification of activities and resulting in false positives or missed falls. This study introduces a novel coordinate system called "ground-face," which is designed to be independent of the device's orientation and placement. In this system, the vertical axis is aligned perpendicularly to the Earth, while the device's x-axis is aligned with the individual's direction of movement. To assess the potential of the vertical component of ground-face referenced accelerometer signals for FD, it was compared with the commonly used acceleration magnitude signal. Detailed analysis was conducted using frequently preferred features in FD studies, and fall detection was performed with various classifiers. Comprehensive experiments demonstrated that the vertical component of the ground-face signal effectively characterizes falls, yielding approximately a 2% improvement in detection accuracy. Moreover, the proposed coordinate system is not limited to FD but can also be applied to human activity recognition (HAR) systems. By mitigating orientation-related discrepancies, it reduces the likelihood of misclassification and enhances the overall HAR capabilities.

Keywords: Fall detection, Accelerometer, Device coordinate system, Global coordinate system, Movement direction

1. Introduction

The World Health Organization defines a fall as the involuntary change in position from a person's current location to a lower position, such as the ground. It is reported that each year, falls lead to 684,000 deaths, making it the second-largest cause of accidental death after road traffic accidents. In addition to fatal falls, there are 37.3 million severe falls requiring medical intervention annually, which can result in lasting injuries [1]. Furthermore, treatments after falls are among the most costly medical interventions [2]. Considering that the risk of falls and severe consequences is higher in elderly individuals and the global elderly population is increasing, falls emerge as a growing issue.

Approximately 12% of the world's population is comprised of individuals over the age of 60, and it is projected that this proportion will reach 16% by the year 2030 and 22% by 2050 [3]. Aging brings about physical, sensory, and cognitive changes that increase the likelihood of falling. Serious injuries or fatalities due to falls are frequently observed among elderly individuals. For instance, in the United States, 20-30% of elderly individuals who experience falls suffer from moderate to severe injuries such as bruises, hip fractures, or head trauma [1]. Every year, 28% of individuals aged 65 and above, as well as 32% of those aged 70 and above, experience falls. Moreover, the elderly constitute the demographic most affected by fatal falls [4].

To address this significant health threat, extensive efforts are being dedicated to systems equipped with automatic fall detection (FD) and alert functions. Automatic FD systems are capable of identifying falls and promptly alerting hospitals or caregivers [5]–[13]. These systems have the potential to reduce the time between a fall and medical intervention, thereby minimizing health complications related to falls.

FD systems primarily use two approaches – wearable-based and environment-based – to distinguish between falls and daily activities. The environment-based method employs technologies such as cameras, infrared cameras, Kinect sensors, microphones, motion, radar, pressure, and vibration sensors. Meanwhile, the wearable-based approach incorporates sensors

Cite as: A. T. Sözer, "Enhancing Fall Detection Accuracy: The Ground-Face Coordinate System for 3D Accelerometer Data," *Sakarya University Journal of Computer and Information Sciences*, vol.7, no. 3, pp. 439-448, 2024. Doi: 10.35377/saucis…1522290

for acceleration, pressure, orientation, magnetic fields, and heart rate monitoring [2], [14]–[22].

Using an inertial measurement unit (IMU), particularly a 3-axis accelerometer, for FD offers advantages such as cost-effectiveness and ease of setup. Furthermore, it is common for human activity recognition (HAR) systems to be equipped with accelerometers. By combining the signals generated by the accelerometer with machine learning approaches, HAR and FD systems with high detection capacity have been developed [23]–[28]. An accelerometer generates signals by detecting the acceleration forces acting along the three axes of the device coordinate system: x, y, and z. It uses internal components like microstructures that respond to physical forces, converting them into electrical signals that can be interpreted as acceleration data. The signals in the device coordinate system make accelerometer signals sensitive to the device's placement and orientation. In simpler terms, when the device is attached in different positions, like on various points on the waist, or during actions such as falling where the device's orientation changes, variation of the acceleration can also be observed in the device's axes that don't align with the direction of movement. Moreover, an accelerometer can exhibit an orientation gap between its package and the physical sensors [29]. This variation in acceleration data due to changes in device placement and orientation introduces a significant limitation for FD and HAR systems. Misalignment between the device's axes and the direction of movement may lead to misinterpretation of acceleration signals, resulting in misclassification of activities, which can cause false positives or missed detections. This makes it critical to develop solutions that compensate for these orientation-induced discrepancies to ensure more accurate detection of falls and other human activities.

A common solution to this issue is often using the norm of the 3D accelerometer signal. This signal, named the acceleration magnitude, is commonly utilized in FD studies and remains unaffected by device placement and orientation [30]–[35]. Another approach to address the aforementioned issue involves expressing accelerometer signals in different coordinate planes. In the global coordinate system, the x-axis becomes tangent to the Earth and points to the East; the y-axis becomes tangent to the Earth but points to the Earth's North Pole; and the z-axis becomes perpendicular to the Earth and points toward the sky. The downward signal obtained by projecting accelerometer signals onto the global coordinate system has been utilized in FD studies [36]–[38]. Another proposed coordinate system is the user-centric coordinate system. In this system, accelerometer signals are first projected onto the global coordinate system and then rotated to user directions calculated from the instantaneous velocity of the user [39].

This study proposes a novel coordinate system named 'ground-face' for potential use in FD and HAR studies. In this system, the vertical axis becomes perpendicular to the Earth, akin to the global coordinate system, while the device's x-axis is aligned with the person's direction. During the study, accelerometer signals referenced to the device were mapped onto this ground-face coordinate system. The FD potential of the resulting downward signal was evaluated by comparing it with the acceleration magnitude. Thorough experiments illustrated that the downward signal more accurately characterizes falls and holds promise for effective FD.

Key contributions of the study:

1. A novel coordinate system has been developed in the proposed framework, where the vertical axis is aligned with the ground, and the x-axis corresponds to the person's direction. This results in a coordinate system that better suits the nature of human movements, regardless of device orientation and placement. As a result, it is well-suited for HAR and FD.
2. A method has been proposed to calculate the angular gap between a person's direction and the device's orientation.
3. The appropriateness of the proposed coordinate system for FD has been affirmed through a comprehensive comparison between the downward signal and the acceleration magnitude.

The subsequent sections of this article are organized as follows: Section II elaborates on the detailed introduction of the projection of device-referenced signals onto the proposed coordinate system and its application in FD. Section III presents a comprehensive performance evaluation. Section IV delves into the experimental findings and the merits and limitations of the suggested coordinate system. Section V concludes the article, offering insights into future work.

2. Materials & Methods

In this section, the calculation of the ground-referenced accelerometer signal is provided. Subsequently, the tools necessary to assess the suitability of the acquired signal for FD are elucidated.

2.1. Ground-Face Coordinate System

The signals generated by 3D accelerometer devices encompass both dynamic and static components. The dynamic component originates from movement, while the static component arises due to the Earth's gravitational force. These signals are produced by accelerometer devices with reference to device coordinate systems. Given their device-referenced nature, during scenarios involving orientation changes such as falls, dynamic and static accelerations manifest in different axes due to the person's orientation (Figure 1(a)). Additionally, the placement of the device could lead to a discrepancy between the direction of movement and the device's orientation. Analyzing these acceleration signals as ground-face referenced instead of device-referenced can offer greater insights into the occurrence of a fall event. Figure 1(b) displays the suggested ground-face coordinate system.

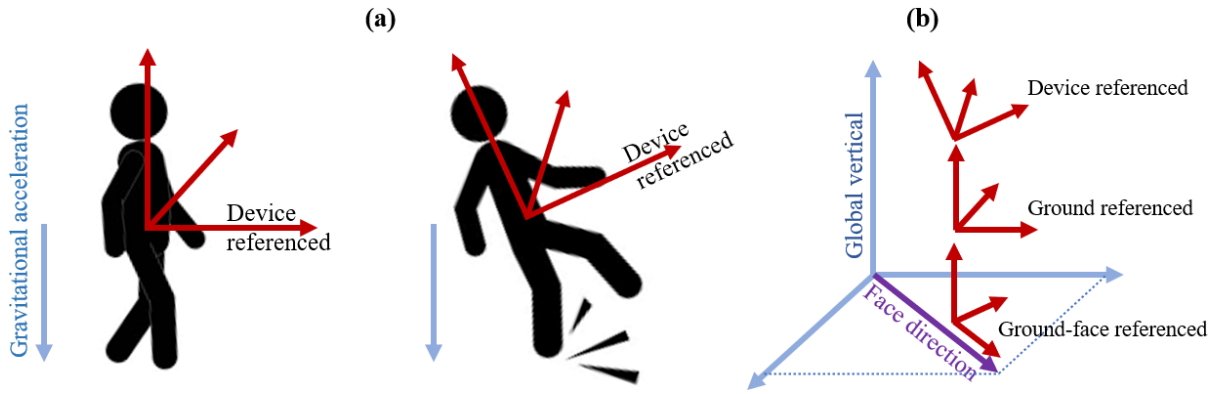

Figure 1. Proposed Ground-Face Coordinate System. (a) Impact of Rotation (b) Various Coordinate Systems. Raw Acceleration Signals Are Initially in the Device Coordinate Systems. In the Ground Coordinate Systems, the x-y Plane Lies Parallel to the Earth's Surface. In the Suggested Ground-Face Coordinate System, the x-y Plane Also Remains Parallel to the Earth's Surface, But the x-axis Aligns with the Direction of the User's Face.

Ground-face referenced signals are derived from signals referenced to the device through a transformation process.

$$A' = RA^T \tag{1}$$

Here $A = [a_x, a_y, a_z]$ holds the accelerometer readings along the device-referenced x, y, and z axes. R represents the rotation matrix, and $A' = [a'_x, a'_y, a'_z]$ denotes the transformed accelerometer values. In a three-dimensional context, the rotation matrix R is composed of three-axis rotations, $R_x(\psi), R_y(\theta), R_z(\beta)$, which are defined by Euler angles. The rotation matrix R is

$$R = R_z(\beta)R_y(\theta)R_x(\psi) \tag{2}$$

The angles ψ and θ can be calculated through sensor fusion involving the accelerometer and gyroscope at each time step. On the other hand, the β angle, a fixed value, is intended to align the device direction with the movement direction. To estimate the angle β, a calibration process is required. During this process, a person performs a straight walk. The estimation of this angle relies on determining the device's direction using principal component analysis (PCA). PCA identifies the axis along which the most significant variation occurs. During a straight walk, the direction of maximum variance calculated by PCA will correspond to the direction of the device, as the largest changes are expected to be in the forward (face) direction. The difference between the face direction and the device's direction yields the angle β which is calculated as follow:

$$\beta = cos^{-1}\frac{\langle \hat{x}, pc \rangle}{||\hat{x}||_2 ||pc||_2} \tag{3}$$

Here, $\hat{x}$ represents a unit vector in the x-direction, which is [1 0], and pc is the principal component of $R_y(\theta)R_x(\psi)a_x^T$ and $R_y(\theta)R_x(\psi)a_y^T$ which correspond to the ground-referenced x and y axes components.

In summary, the device-referenced x and y-axis signals are transformed into ground-referenced format, and the angle β is determined with the help of PCA.

As a result of the transformation, the signals a'_x and a'_y respectively carry information about the forward and lateral components of a person's movement, whereas the signal a'_z provides information about components perpendicular to the ground. The signals in A' can be utilized for HAR and FD.

2.2. Relevant Features for Fall Detection

To demonstrate the functionality of A' for FD, a comparison between device referenced and ground-face referenced accelerometer signals was necessary. The sum vector magnitude, $||\boldsymbol{a}|| = \sqrt{a_x^2 + a_y^2 + a_z^2}$, is frequently employed in accelerometer-based FD algorithms. This choice of signal is primarily due to its independence from device position and orientation. On the other hand, in the ground-referenced signal, fall-related information is carried by downward signal, a'_z. Hence, a comparison was made between a'_z and $||\boldsymbol{a}||$ in terms of the insights they provided into the fall event.

Illustrated in Figure 2, the timeframe consisting of one second before the peak and the subsequent 0.3 seconds has been identified as the critical phase. For the purpose of comparison, we selected several features: maximum, minimum, and vertical displacement during the pre-impact phase, range, standard deviation of the critical phase, and maximum falling speed.

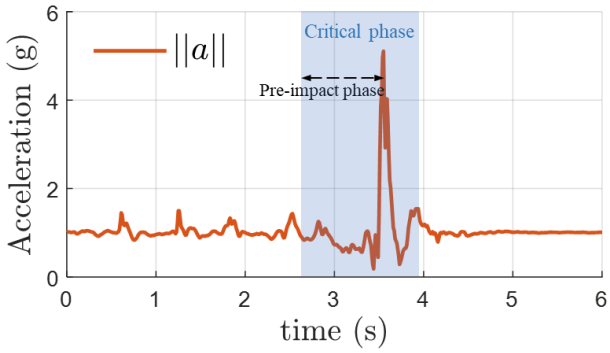

Figure 2. The Phases of Falls Utilized for Feature Extraction

2.3. Assessment Criteria

To assess the information carried out by each feature related to the fall event, Mutual Information Criteria (MIC) values were obtained. The mutual information quantifies the amount of knowledge a feature offers regarding the fall event. For each feature, Receiver Operating Characteristic (ROC) curves were plotted, illustrating the trade-off between sensitivity (fall detection capacity) and specificity (capacity to avoid wrong fall alarm performance). Furthermore, Area Under the Curve (AUC) values, which indicate the overall performance of a binary classification model by calculating the area under the ROC curve, were computed.

Additionally, the signals were compared to the classification accuracy achieved by machine learning models. Support Vector Machine (SVM), k-Nearest Neighbors (KNN), and Random Forest (RF) algorithms were employed, and values for sensitivity, specificity, and accuracy were obtained.

2.4. Dataset

The proposed ground-face reference system has been tested with a public, extensive fall dataset, KFall [40]. The dataset was obtained from 32 young participants who performed 21 activities of daily living (ADLs) and 15 types of falls. An inertial sensor was attached to their lower back to capture the movements. The dataset comprises 5075 motion files, including 2729 ADL and 2346 fall events. Each file provides acceleration, angular velocity, and Euler angle samples along three axes.

3. Experimental Results

The proposed method was tested by rotating the device-referenced signal to the ground-face reference system and its usage on FD.

3.1. Calibration Stage

Accelerometer signals referenced to the ground-face coordinate system were captured during the calibration phase. This phase involved measuring acceleration and orientation angles during straight walks. An individual positioned an Android mobile phone on their waist at various angles and performed straight-line walks. The phone was placed at five different angles, and the individual completed five 5-second walks. Acceleration data, along with the rotation angles ψ and θ, were recorded from the phone. Figure 3 shows the Android device's axes and the corresponding acceleration measurements.

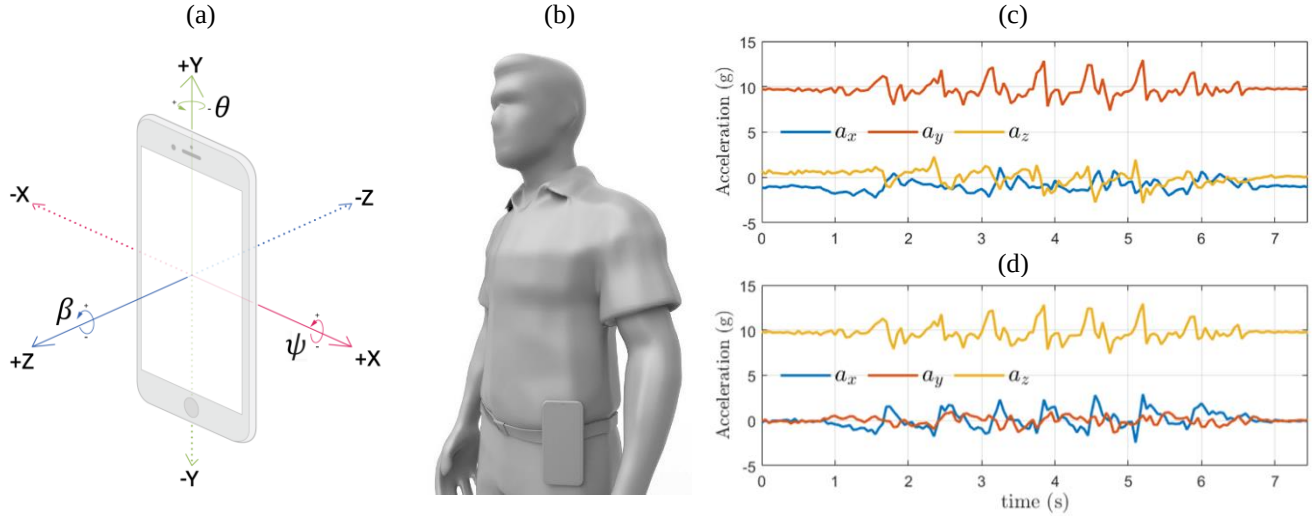

Figure 3. Calibration Experiments. (a) Android Device Axes for Acceleration and Rotation. (b) The Device Placed at Various Angles on the Individual's Waist. (c) Acceleration Signals Relative to the Device, with Average Rotation Angles of $\psi = -89°$ and $\theta = -6°$. (d) Ground-Face-Referenced Acceleration Signals, with Gravity Observed Solely on the Z-Axis. The Calculated β Angle was 63°.

Ground-referenced signals were obtained from the acceleration values and ψ and θ rotation angles measured from the phone positioned at angles around the waist as specified by Real β in Table 1. Using these values, the β angles shown in Table 1 were calculated, where 0° corresponds to the right side of the waist and 180° to the left side. A review of Table 1 reveals that the calculated values are very close to the real values. In Figure 3(d), examining the x and y components of the ground-face referenced accelerometer signal indicates that the forward movement during walking is reflected in the x-axis.

Table 1. Real and Calculated β Angles

Real β	15°	55°	90°	115°	155°
Calculated β	$9.5° \pm 4.7°$	$56.6° \pm 5.1°$	$90.1° \pm 4°$	$113.8° \pm 1.8°$	$162.8° \pm 6.6°$

3.2. FD by Downward Signal

The downward signal, perpendicular to the Earth in the ground-face referenced acceleration signals, was analyzed for its FD potential by comparing it to the acceleration magnitude. The accelerometer signals during a fall are depicted in Figure 4. Device-referenced signals are shown in Figure 4 (a), while ground-face referenced signals obtained through transformation are shown in Figure 4 (b). In Figure 4 (c), the acceleration magnitude, $||\boldsymbol{a}||$, is illustrated, and in Figure 4 (d), the downward signal, a'_z, signal is depicted. In Figure 4 (a), a high magnitude is visible along the y-axis during impact, while in Figure 4 (b), a high magnitude is observed along the z-axis. Upon comparing Figure 4 (c) & (d), it becomes apparent that the acceleration change during a fall is more pronounced in the a'_z signal.

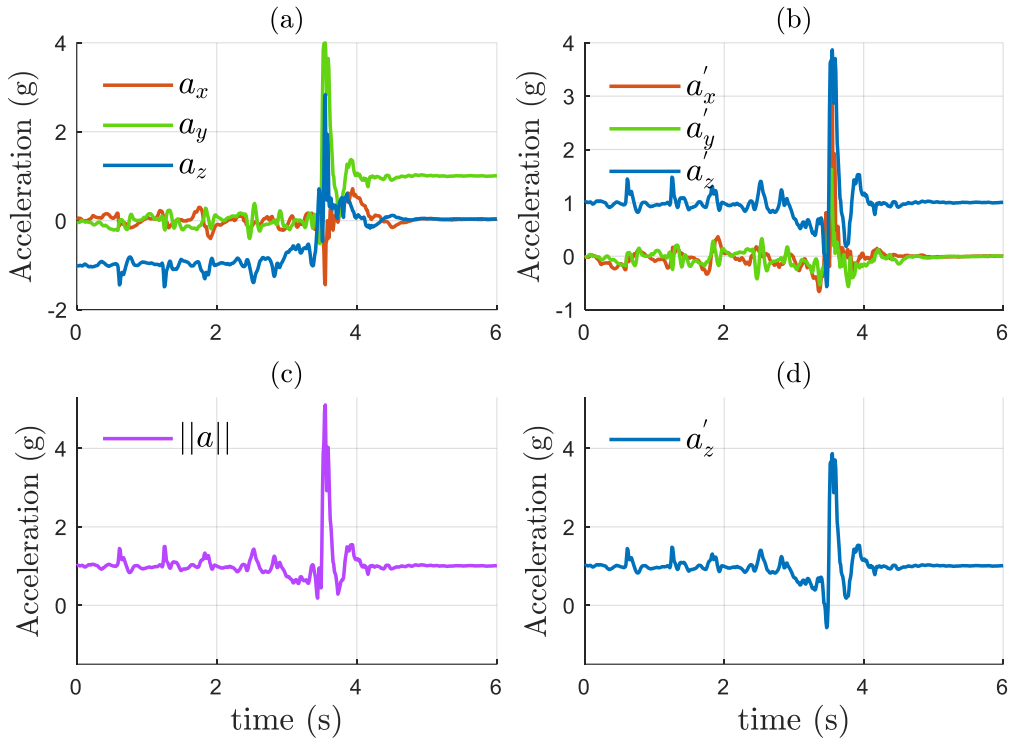

Figure 4. Device and Ground-Face Referenced Accelerometer Signals During a Lateral Fall While Walking. (a) Device Referenced One (b) Ground-Face Reference One (C) Acceleration Magnitude (D) Downward Signal

Detailed analyses and FD detection were performed using the feature values obtained for $||\boldsymbol{a}||$ and a'_z during the critical phase, and the results are presented in the following tables and graphs. In Table 2, you can see the MIV and AUC values derived from $||\boldsymbol{a}||$ and a'_z. In the results of both metrics, it's evident that the a'_z signal better represents falls. Notably, there is a significant difference in MIV and AUC values for the vertical displacement and max falling speed features.

Table 2. The MIV and AUC Values Obtained from the Acceleration Magnitude and Downward Signals

	Mutual Information Value		**Area Under Curve**	
Feature	$\|\|\boldsymbol{a}\|\|$	a'_z	$\|\|\boldsymbol{a}\|\|$	a'_z
Max	0.370	0.367	0.936	0.934
Min	0.181	0.260	0.759	0.839
Range	0.344	0.345	0.920	0.919
Standard deviation	0.337	0.336	0.893	0.856
Vertical displacement	0.184	**0.305**	0.831	**0.907**
Max falling speed	0.331	**0.502**	0.920	**0.981**

In Figure 5 (a), the vertical displacement feature is depicted in a scatter plot, while in Figure 5 (b), the max falling speed feature is presented. As evident from the figures, it can be observed that the attributes derived from a'_z provide better discrimination between ADL and fall samples.

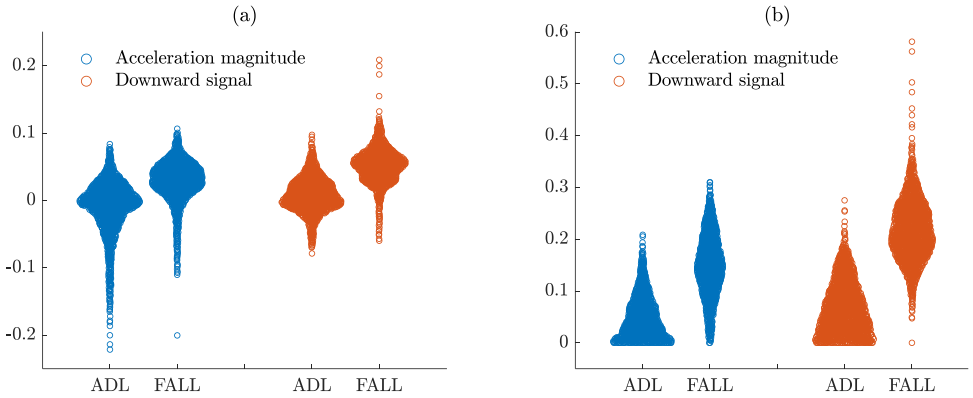

Figure 5. The Distribution of Features Obtained from Acceleration Magnitude and a'_z (a) Vertical Displacement (b) Maximum Falling Speed.

In Figure 6, ROC curves for each feature are displayed. The curves represent the sensitivity and specificity values obtained using the SVM classifier. When each feature is individually assessed, it becomes evident that the features derived from the a'_z signal carries equal or more fall-related information.

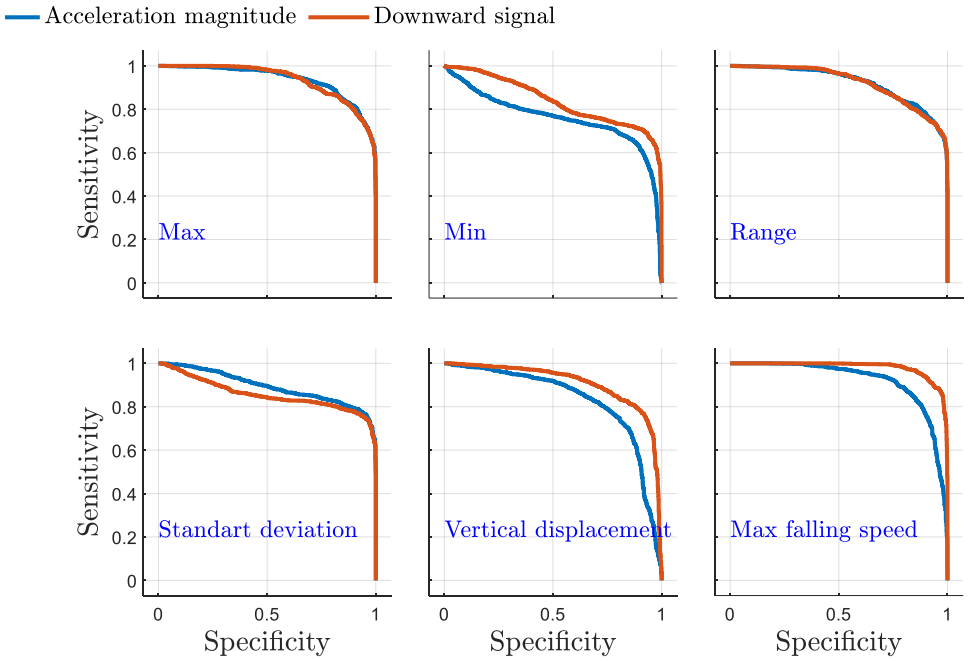

Figure 6. ROC Curves for Each Feature Obtained from Acceleration Magnitude and a'_z

Classification results using $||\boldsymbol{a}||$, a'_z and both together are shown in Table 3. Set1 represents the features derived from the $||\boldsymbol{a}||$, while Set2 represents the features derived from the a'_z. Set3 is the combination of Set1 and Set2. The results were obtained using the leave-subjects-out cross-validation approach, where in each trial, half of the subjects were chosen for training and the remaining half for testing.

Table 3. Performance Evaluation Using Various Classifiers and Feature Sets

	ACCURACY (%)			SENSITIVITY (%)			SPECIFICITY (%)		
	SET1	SET2	SET3	SET1	SET2	SET3	SET1	SET2	SET3
SVM	95.51	95.55	**97.15**	96.06	95.15	**97.03**	95.05	95.89	**97.25**
KNN	95.01	94.86	**96.26**	94.94	94.65	**95.71**	95.06	95.04	**96.72**
RF	95.27	95.41	**96.28**	95.38	95.48	**96.10**	95.18	95.34	**96.43**

Upon examining the results, it is observed that the accuracy values obtained from Set1 and Set2 are approximately the same. However, Set1 provides higher sensitivity compared to Set2, while Set2 offers higher specificity values. The combination of all features extracted from both signals has led to a significant improvement in classification performance, resulting in an increase of approximately 2% with SVM.

In order to better assess the influence of the a'_z signal on FD detection, the results of SVM classifier for each activity and fall type are displayed in Figure 7. The figure demonstrates that a'_z is particularly capable of more accurately representing certain falls and activities.

4. Discussion

Due to its advantages, such as portability and low power consumption, accelerometers are commonly preferred for FD problems. Accelerometer devices present signals in a device-referenced manner. This device-referenced signal presentation can provide information about the person's orientation, whether vertical or horizontal. However, during a fall, the individual's rotation can change, causing the downward motion-induced acceleration changes to be shared across the x, y, and z axes. Consequently, device-referenced signals may not accurately reflect downward motion. In this study, it is claimed that when the x-y plane is consistently parallel to the ground surface, acceleration values will better reflect downward motion and thus carry more information for FD.

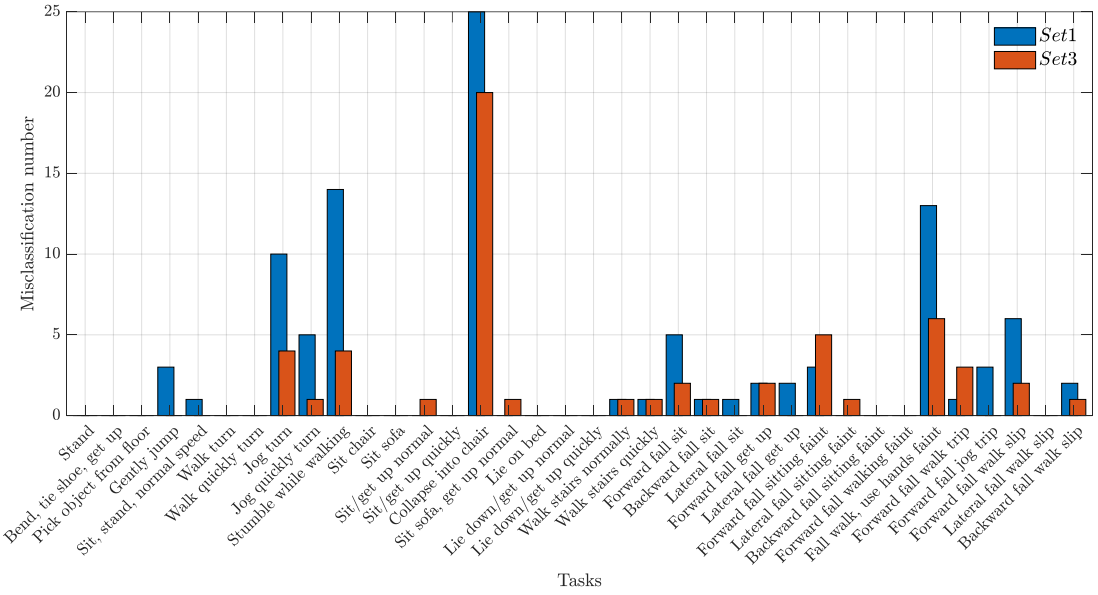

Figure 7. The Misclassification Counts of the SVM Classifier Using Set1 and Set3 for Each Activity and Fall Type in the Dataset

To address this issue, a ground-face coordinate system has been proposed. In this system, the x-y plane remains consistently parallel to the ground surface, while the z-axis remains perpendicular to the ground. In the study, ground-face referenced signals were derived from device referenced signals through a rotation process. The potential of these derived signals in FD has been investigated. For a fair evaluation, the information provided by the commonly preferred $||a||$ signal and the transformed a'_z signal regarding fall events, as well as their suitability for FD, have been extensively compared. The results of this detailed comparison are presented in the Experimental Results section.

When examining the MIV and AUC values for each feature in the table, it is evident that features derived from the a'_z signal yield either comparable or significantly better results. Notably, the downward maximum speed attribute exhibits a strong discriminative characteristic concerning fall events. Furthermore, the ROC curves depicting the trade-off between sensitivity and specificity for each feature also exhibit promising outcomes for FD using the a'_z signal.

When examining the classification results obtained with feature sets Set1, Set2, and Set3, it becomes apparent that Set1 and Set2 yield similar outcomes, while Set3 demonstrates a noteworthy increase in accuracy by up to 2%. A closer look at the sensitivity and specificity values on the Figure 8 reveals an interesting pattern: Set1 exhibits higher sensitivity, whereas Set2 showcases higher specificity. This implies that Set1 is more adept at detecting falls, while Set2 excels in recognizing non-fall situations. The integration of Set3 significantly enhances both sensitivity and specificity values. Based on this observation, it can be inferred that combining the $||a||$ signal with the a'_z signal is more suitable for FD. Figure 7 validates the recommendation to use the $\left|\left|a\right|\right|$ and a'_z signals together for FD. Notable reductions in the misclassification of daily activities and falls, such as 'Jog with turn', 'Stumble while walking', and 'Sit for a moment, attempting to rise, and then collapsing into a chair,' were observed. This suggests that the a'_z signal may represent certain activities more effectively.

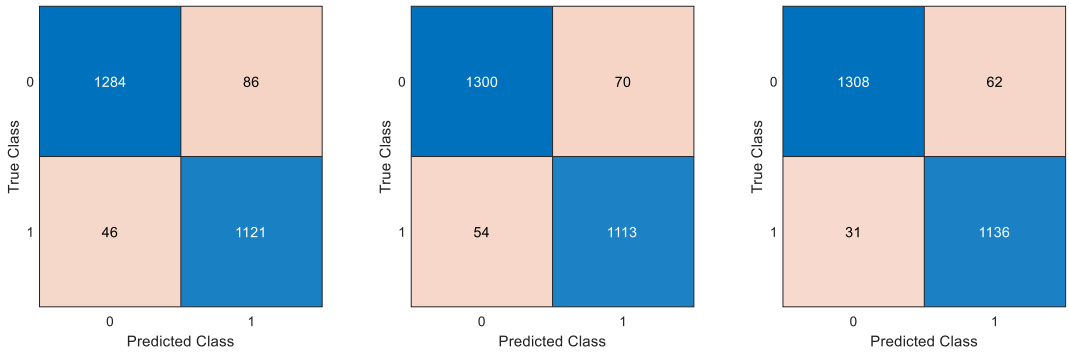

Figure 8. Comparing the Accuracy Levels Among Set1, Set2, and Set3

Regarding the difference between the proposed method and other coordinate systems: In the global coordinate system, the x-axis represents the east direction, and the y-axis points to the north pole. This leads to the x and y-axis signals being dependent on the direction of movement. In FD and HAR studies using the global coordinate system, the components of motion in the east and north pole directions do not carry any specific meaning related to the nature of the motion. In the user-centric coordinate system, the y-axis aligns with the user's direction. However, since the user's direction is estimated based on the instantaneous velocity in the 3D space, this method is more susceptible to device rotations and noise.

One limitation of the proposed method is that the performance improvements obtained from each feature did not repeat when these features were used together. This discrepancy could be limited information carried by the a'_z signal concerning ADLs. Considering the ground-face referenced signals parallel to the Earth's surface may enhance FD performance.

Another constraint of the suggested approach is its dependence on momentary angle values during the transformation process, necessitating the use of both accelerometer and gyroscope devices. In FD systems, using only accelerometers can lead to lower-cost systems at the expense of performance. However, the proposed method requires gyroscope data due to the need to express accelerometer data in a different coordinate system based on angle values. Additionally, the proposed system requires a 3x3 matrix multiplication for each measured acceleration value. Although this step is performed only once, the calibration stage increases the computational load. Thus, there is a trade-off between FD performance and cost. For systems where the FD process is performed on a computer, this computational load can be negligible, but it must be considered for embedded systems.

It should be noted that ground-face referenced signals do not replace device-referenced signals; rather, they provide additional information. This allows for more comprehensive analyses, leading to more successful FD and HAR systems.

5. Conclusion

In this study, a novel coordinate system called ground face coordinate system is proposed for accelerometer signals that can be used in IMU-based HAR and FD studies. The effectiveness of the downward signal obtained is tested in the FD problem.

Comparative experiments using the commonly preferred $||\boldsymbol{a}||$ signal in accelerometer-based FD studies have demonstrated that the use of the downward signal increases the correct detection of falls and daily activities around %2. Thus, the downward signal provides more distinctive information about falls. Therefore, the proposed coordinate system has the potential to enhance performance in both HAR and FD studies.

In future research, incorporating the evaluation of signals parallel to the ground obtained through the proposed transformation could lead to more successful systems.

References

[1] World Health Organization, “Step safely: Strategies for preventing and managing falls across the life-course,” GENEVA.

[2] R. Rajagopalan, I. Litvan, and T. P. Jung, “Fall prediction and prevention systems: Recent trends, challenges, and future research directions,” *Sensors (Switzerland)*, vol. 17, no. 11, pp. 1–17, 2017.

[3] United Nations, “World Population Ageing 2019,” New York.

[4] K. C. Liu, C. Y. Hsieh, H. Y. Huang, S. J. P. Hsu, and C. T. Chan, “An Analysis of Segmentation Approaches and Window Sizes in Wearable-Based Critical Fall Detection Systems with Machine Learning Models,” *IEEE Sens. J.*, vol. 20, no. 6, pp. 3303–3313, 2020.

[5] J. Marques and P. Moreno, “Online Fall Detection Using Wrist Devices,” *Sensors*, vol. 23, no. 3, 2023.

[6] T. Huang, M. Li, and J. Huang, “Recent trends in wearable device used to detect freezing of gait and falls in people with Parkinson’s disease: A systematic review,” *Front. Aging Neurosci.*, vol. 15, 2023.

[7] E. A. De La Cal, M. Fáñez, M. Villar, J. R. Villar, and V. M. González, “A low-power HAR method for fall and high-intensity ADLs identification using wrist-worn accelerometer devices,” *Log. J. IGPL*, vol. 31, no. 2, pp. 375–389,

2023.
[8] P. Bhattacharjee, S. Biswas, S. Chattopadhyay, S. Roy, and S. Chakraborty, "Smart Assistance to Reduce the Fear of Falling in Parkinson Patients Using IoT," *Wirel. Pers. Commun.*, vol. 130, no. 1, pp. 281–302, 2023.
[9] H.-C. Lin, M.-J. Chen, C.-H. Lee, L.-C. Kung, and J.-T. Huang, "Fall Recognition Based on an IMU Wearable Device and Fall Verification through a Smart Speaker and the IoT," *Sensors*, vol. 23, no. 12, 2023.
[10] A. Alqahtani, S. Alsubai, M. Sha, V. Peter, A. S. Almadhor, and S. Abbas, "Falling and Drowning Detection Framework Using Smartphone Sensors," *Comput. Intell. Neurosci.*, vol. 2022, 2022.
[11] B. Brew, S. G. Faux, and E. Blanchard, "Effectiveness of a Smartwatch App in Detecting Induced Falls: Observational Study," *JMIR Form. Res.*, vol. 6, no. 3, 2022.
[12] M. E. Issa, A. M. Helm, M. A. A. Al-Qaness, A. Dahou, M. A. Elaziz, and R. Damaševičius, "Human Activity Recognition Based on Embedded Sensor Data Fusion for the Internet of Healthcare Things," *Healthc.*, vol. 10, no. 6, 2022.
[13] A. N. Pereira *et al.*, "Flexible Sensor Suite Integrated into Textile for Calcium Ion and Fall Detection," *IEEE Sensors Lett.*, vol. 6, no. 10, 2022.
[14] Y. H. Nho, J. G. Lim, and D. S. Kwon, "Cluster-Analysis-Based User-Adaptive Fall Detection Using Fusion of Heart Rate Sensor and Accelerometer in a Wearable Device," *IEEE Access*, vol. 8, pp. 40389–40401, 2020.
[15] M. Saleh and R. L. B. Jeannes, "Elderly Fall Detection Using Wearable Sensors: A Low Cost Highly Accurate Algorithm," *IEEE Sens. J.*, vol. 19, no. 8, pp. 3156–3164, 2019.
[16] C. Wang *et al.*, "Low-Power Fall Detector Using Triaxial Accelerometry and Barometric Pressure Sensing," *IEEE Trans. Ind. Informatics*, vol. 12, no. 6, pp. 2302–2311, 2016.
[17] X. Wang, J. Ellul, and G. Azzopardi, "Elderly Fall Detection Systems: A Literature Survey," *Front. Robot. AI*, vol. 7, no. June, 2020.
[18] J. L. Chua, Y. C. Chang, and W. K. Lim, "A simple vision-based fall detection technique for indoor video surveillance," *Signal, Image Video Process.*, vol. 9, no. 3, pp. 623–633, 2015.
[19] M. G. Amin, Y. D. Zhang, F. Ahmad, and K. C. D. Ho, "Radar signal processing for elderly fall detection: The future for in-home monitoring," *IEEE Signal Process. Mag.*, vol. 33, no. 2, pp. 71–80, 2016.
[20] B. Kwolek and M. Kepski, "Human fall detection on embedded platform using depth maps and wireless accelerometer," *Comput. Methods Programs Biomed.*, vol. 117, no. 3, pp. 489–501, 2014.
[21] Y. Wang, K. Wu, and L. M. Ni, "WiFall: Device-Free Fall Detection by Wireless Networks," *IEEE Trans. Mob. Comput.*, vol. 16, no. 2, pp. 581–594, 2017.
[22] S. K. Gharghan and H. A. Hashim, "A comprehensive review of elderly fall detection using wireless communication and artificial intelligence techniques," *Measurement*, vol. 226, p. 114186, Feb. 2024.
[23] P. Kumar, S. Chauhan, and L. K. Awasthi, "Human Activity Recognition (HAR) Using Deep Learning: Review, Methodologies, Progress and Future Research Directions," *Arch. Comput. Methods Eng.*, Aug. 2023.
[24] L. Minh Dang, K. Min, H. Wang, M. Jalil Piran, C. Hee Lee, and H. Moon, "Sensor-based and vision-based human activity recognition: A comprehensive survey," *Pattern Recognit.*, vol. 108, p. 107561, Dec. 2020.
[25] L. Palmerini, J. Klenk, C. Becker, and L. Chiari, "Accelerometer-based fall detection using machine learning: Training and testing on real-world falls," *Sensors (Switzerland)*, vol. 20, no. 22, pp. 1–15, 2020.
[26] N. Pannurat, S. Thiemjarus, and E. Nantajeewarawat, "Automatic fall monitoring: A review," *Sensors (Switzerland)*, vol. 14, no. 7, pp. 12900–12936, 2014.
[27] S. Nooruddin, M. M. Islam, F. A. Sharna, H. Alhetari, and M. N. Kabir, "Sensor-based fall detection systems: A review," *J. Ambient Intell. Humaniz. Comput.*, vol. 13, no. 5, pp. 2735–2751, 2022.
[28] J. A. Santoyo-Ramón, E. Casilari, and J. M. Cano-García, "A study of one-class classification algorithms for wearable fall sensors," *Biosensors*, vol. 11, no. 8, pp. 1–20, 2021.
[29] H. Kimura, M. Nakamura, N. Inou, M. Matsudaira, and M. Yoshida, "Identification Method of Sensor Directions and Sensitivities in Multi-Axis Accelerometer (Actual Measurement of Direction Tensor and Sensitivity Tensor)," *J. Robot. Mechatronics*, vol. 25, no. 2, pp. 408–416, Apr. 2013.
[30] J. R. Villar, C. Chira, E. de la Cal, V. M. González, J. Sedano, and S. B. Khojasteh, "Autonomous on-wrist acceleration-based fall detection systems: Unsolved challenges," *Neurocomputing*, vol. 452, pp. 404–413, 2021.
[31] M. Abbas and R. L. B. Jeannes, "Exploiting Local Temporal Characteristics via Multinomial Decomposition Algorithm for Real-Time Activity Recognition," *IEEE Trans. Instrum. Meas.*, vol. 70, 2021.
[32] G. Šeketa, L. Pavlaković, D. Džaja, I. Lacković, and R. Magjarević, "Event-Centered Data Segmentation in Accelerometer-Based Fall Detection Algorithms," *Sensors*, vol. 21, no. 13, p. 4335, Jun. 2021.
[33] C. Mosquera-Lopez *et al.*, "Automated Detection of Real-World Falls: Modeled from People with Multiple Sclerosis," *IEEE J. Biomed. Heal. Informatics*, vol. 25, no. 6, pp. 1975–1984, 2021.
[34] M. J. Al Nahian *et al.*, "Towards an Accelerometer-Based Elderly Fall Detection System Using Cross-Disciplinary Time Series Features," *IEEE Access*, vol. 9, pp. 39413–39431, 2021.
[35] M. Saleh, M. Abbas, and R. B. Le Jeannes, "FallAllD: An Open Dataset of Human Falls and Activities of Daily Living for Classical and Deep Learning Applications," *IEEE Sens. J.*, vol. 21, no. 2, pp. 1849–1858, 2021.
[36] Y. Yan and Y. Ou, "Accurate fall detection by nine-axis IMU sensor," *2017 IEEE Int. Conf. Robot. Biomimetics, ROBIO 2017*, vol. 2018-Janua, pp. 1–6, 2018.

[37] M. M. Musngi, O. Aziz, S. Zihajehzadeh, G. C. Nazareth, C. G. Tae, and E. J. Park, "Use of Average Vertical Velocity and Difference in Altitude for Improving Automatic Fall Detection from Trunk Based Inertial and Barometric Pressure Measurements," *Proc. Annu. Int. Conf. IEEE Eng. Med. Biol. Soc. EMBS*, vol. 2018-July, pp. 5146–5149, 2018.
[38] J. K. Lee, S. N. Robinovitch, and E. J. Park, "Inertial Sensing-Based Pre-Impact Detection of Falls Involving Near-Fall Scenarios," *IEEE Trans. Neural Syst. Rehabil. Eng.*, vol. 23, no. 2, pp. 258–266, 2015.
[39] A. Ferreira, G. Santos, A. Rocha, and S. Goldenstein, "User-Centric Coordinates for Applications Leveraging 3-Axis Accelerometer Data," *IEEE Sens. J.*, vol. 17, no. 16, pp. 5231–5243, 2017.
[40] X. Yu, J. Jang, and S. Xiong, "A Large-Scale Open Motion Dataset (KFall) and Benchmark Algorithms for Detecting Pre-impact Fall of the Elderly Using Wearable Inertial Sensors," *Front. Aging Neurosci.*, vol. 13, Jul. 2021.

Author(s) Contributions
The article is written by a single author. I hereby declare that I have prepared the article alone for the authorship declaration.

Conflict of Interest Notice
The author declares that there are no potential conflicts of interest.

Ethical Approval
It is declared that during the preparation process of this study, scientific and ethical principles were followed, and all the studies benefited from are stated in the bibliography.

Availability of data and material
The datasets analyzed during the current study are available from https://sites.google.com/view/kfalldataset/

Plagiarism Statement
This article has been scanned by iThenticate ™.